Failure to ubiquitinate c-Met leads to hyperactivation of mTOR signaling in a mouse model of autosomal dominant polycystic kidney disease

Shan Qin,[1,2] Mary Taglienti,[1,2] Surya M. Nauli,[3] Leah Contrino,[3] Ayumi Takakura,[3] Jing Zhou,[3] and Jordan A. Kreidberg[1,2]

[1]Department of Medicine, Children's Hospital Boston, and Department of Pediatrics, Harvard Medical School, Boston, Massachusetts, USA. [2]Harvard Stem Cell Institute, Cambridge, Massachusetts, USA. [3]Department of Medicine, Brigham and Women's Hospital, and Department of Medicine, Harvard Medical School, Boston, Massachusetts, USA.

Autosomal dominant polycystic kidney disease (ADPKD) is a common inherited disorder that is caused by mutations at two loci, polycystin 1 (*PKD1*) and polycystin 2 (*PKD2*). It is characterized by the formation of multiple cysts in the kidneys that can lead to chronic renal failure. Previous studies have suggested a role for hyperactivation of mammalian target of rapamycin (mTOR) in cystogenesis, but the etiology of mTOR hyperactivation has not been fully elucidated. In this report we have shown that mTOR is hyperactivated in *Pkd1*-null mouse cells due to failure of the HGF receptor c-Met to be properly ubiquitinated and subsequently degraded after stimulation by HGF. In *Pkd1*-null cells, Casitas B-lineage lymphoma (c-Cbl), an E3-ubiquitin ligase for c-Met, was sequestered in the Golgi apparatus with $\alpha_3\beta_1$ integrin, resulting in the inability to ubiquitinate c-Met. Treatment of mouse *Pkd1*-null cystic kidneys in organ culture with a c-Met pharmacological inhibitor resulted in inhibition of mTOR activity and blocked cystogenesis in this mouse model of ADPKD. We therefore suggest that blockade of c-Met is a potential novel therapeutic approach to the treatment of ADPKD.

Introduction

Polycystic kidney disease (PKD) is one of the most common inherited disorders that result in severe and debilitating disease. There are two predisposing loci, *PKD1* and *PKD2*, residing on chromosomes 16 and 4, respectively (1, 2), which encode polycystin-1 and polycystin-2. Extensive study of polycystins and associated proteins has begun to elucidate the molecular biology of cystogenesis (3). Nevertheless, the precise molecular mechanisms of cyst formation remain to be determined.

Several primary pathogenetic mechanisms have been considered to be responsible for cyst formation, including: (a) abnormal regulation of epithelial cell proliferation (4–6); (b) abnormal transepithelial transport resulting in fluid accumulation in tubular lumina (7, 8); and (c) remodeling of the ECM, leading to abnormal epithelial morphology, proliferation, and/or survival (9–11). Several signal transduction pathways are known to regulate epithelial cell expansion during kidney development, including those downstream of c-Ret (12) and of receptors for FGFs (13, 14) and bone morphogenetic proteins (BMPs) (13). An additional receptor tyrosine kinase, c-Met, is expressed in collecting duct epithelial cells and binds HGF. A role for c-Met in branching morphogenesis within the developing kidney has long been suggested because of the ability of HGF to stimulate the formation of branched tubules by MDCK cells in 3D collagen gels (15, 16). A role for HGF and c-Met in cystic kidney disease has also been suggested by observations that both HGF and c-Met are overexpressed by cyst-lining cells in kidneys from individuals with PKD or acquired cystic disease (6, 17).

Integrin receptors are heterodimeric transmembrane proteins that mediate attachment of cells to the ECM. We previously demonstrated a role for $\alpha_3\beta_1$ integrin in kidney development; targeted mutation of the α_3 integrin gene results in shorter and fewer collecting ducts in mutant kidneys, an observation consistent with decreased branching morphogenesis and/or decreased epithelial tubule expansion (18). Small cysts are also observed in α_3 integrin mutant kidneys, suggesting that $\alpha_3\beta_1$ integrin may have a role in maintaining normal tubular morphology and dysfunction of $\alpha_3\beta_1$ integrin may relate to cystogenesis. Consistent with this finding, a hypomorphic mutation in the mouse laminin α5 gene, which encodes the major ligand for $\alpha_3\beta_1$ integrin, causes a phenotype that resembles PKD (19). A major signaling pathway through which integrins regulate epithelial cell behavior involves PI3K and Akt (20, 21). Mammalian target of rapamycin (mTOR) is one of the major targets of Akt, and increased activation of mTOR has been suggested to contribute to cyst formation in mice and humans (22). How mTOR activity is controlled in PKD is not fully understood.

Here we show that glycosylation of the α_3 integrin subunit is defective and $\alpha_3\beta_1$ integrin is retained in the Golgi apparatus in *Pkd1*$^{-/-}$ cells. Casitas B-lineage lymphoma (c-Cbl), an E3 ubiquitin ligase normally responsible for ubiquitination of c-Met, is also sequestered in the Golgi apparatus with $\alpha_3\beta_1$ integrin in *Pkd1*$^{-/-}$ cells. Consistent with these results, ubiquitination of c-Met after stimulation with HGF is defective in *Pkd1*$^{-/-}$ cells, and there is an increased c-Met–dependent activation of the PI3K/Akt/mTOR signaling pathway. Additionally, pharmacological blockade of c-Met signaling results in a dramatic decrease in cyst formation in *Pkd1*$^{-/-}$ embryos.

Conflict of interest: S. Qin and J.A. Kreidberg have a patent pending based on the results of this article.

Citation for this article: *J Clin Invest.* 2010;120(10):3617–3628. doi:10.1172/JCI41531.

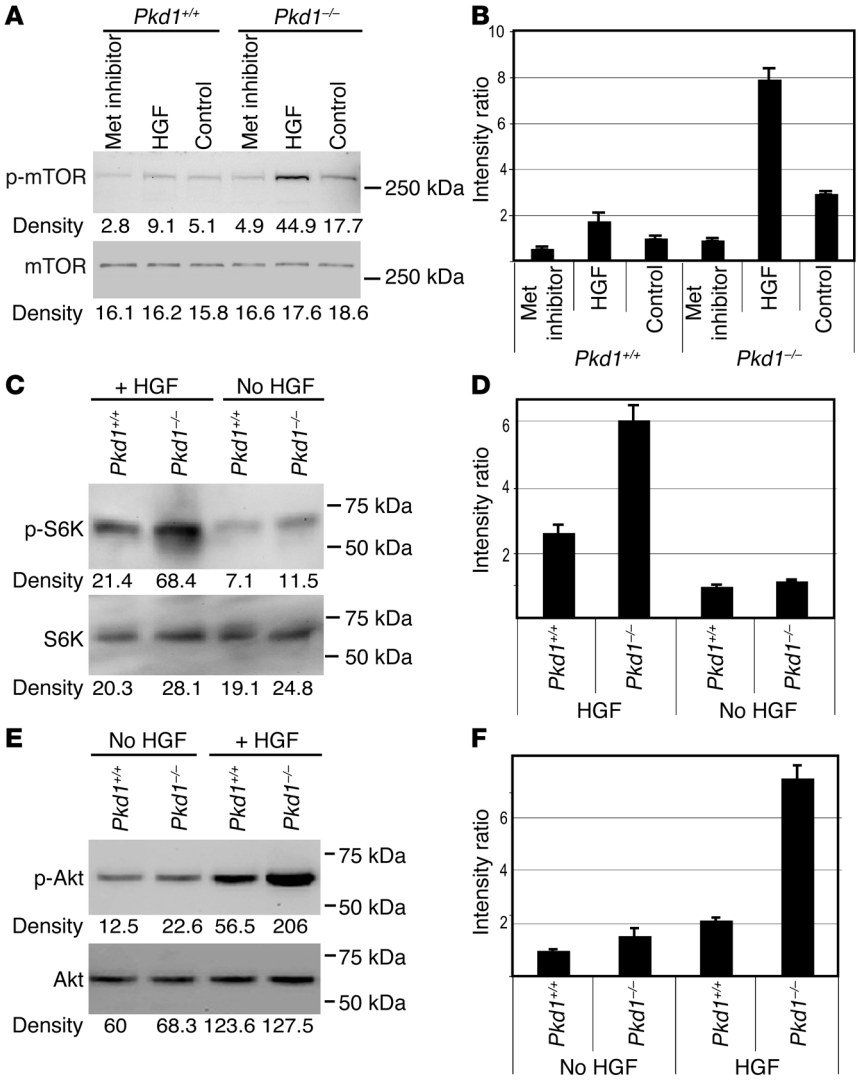

Figure 1
HGF stimulation causes hyper-phosphorylation of mTOR (**A** and **B**), S6K (**C** and **D**), and Akt (**E** and **F**) in *Pkd1*$^{-/-}$ cells. Western blots for phospho-mTOR and mTOR (**A**), phospho-S6K (Thr398) and S6K (**C**), phospho-Akt (Ser473) and Akt (**E**). Densitometry is shown in **B**, **D**, and **F**, and values for each lane are shown below each blot. In all experiments, serum-starved *Pkd1*$^{+/+}$ and *Pkd1*$^{-/-}$ cells were incubated with media alone (control) or media containing HGF (50 ng/ml for 20 minutes). In **A** and **B**, c-Met inhibitor (5 mM for 40 minutes) was also included. (**A** and **B**) mTOR is hyperphosphorylated in *Pkd1*$^{-/-}$ cells, both at steady state and after HGF stimulation; steady-state phosphorylation is sensitive to c-Met inhibitor. (**C** and **D**) S6K (Thr398) is hyperphosphorylated in *Pkd1*$^{-/-}$ cells after stimulation with HGF. (**E** and **F**) Akt is hyperphosphorylated in *Pkd1*$^{-/-}$ cells after stimulation with HGF. All figures are representative of 3 experiments.

Results

Hyperactivation of mTOR in Pkd1$^{-/-}$ *cells is dependent on c-Met.* Consistent with previously published results (22), mTOR and S6K were hyperphosphorylated in an immortalized *Pkd1*$^{-/-}$ cell line derived from E15.5 *Pkd1*$^{-/-}$ kidneys (ref. 23 and Figure 1). Stimulation with HGF accentuated the difference in mTOR and S6K phosphorylation between *Pkd1*$^{-/-}$ and WT (*Pkd1*$^{+/+}$) cells, whereas treatment with a c-Met inhibitor (Met Kinase Inhibitor, Calbiochem) reduced mTOR phosphorylation in *Pkd1*$^{-/-}$ cells to a baseline level observed in WT cells (Figure 1, A–D). HGF-dependent phosphorylation of Akt was also stronger in *Pkd1*$^{-/-}$ cells than in *Pkd1*$^{+/+}$ cells (Figure 1, E and F). These results indicate that hyperactivation of mTOR in PKD may occur downstream of the receptor tyrosine kinase c-Met, and through the c-Met/Akt pathway.

Defective ubiquitination of c-Met in Pkd1$^{-/-}$ *cells.* To elucidate the mechanism whereby HGF stimulation resulted in hyperphosphorylation of mTOR in *Pkd1*$^{-/-}$ cells, we first examined levels of c-Met, Akt, and mTOR in immortalized *Pkd1*$^{-/-}$ and WT cells. Akt and mTOR were present at equivalent levels (Figure 1, A, B, E, and F), whereas c-Met was more abundant in *Pkd1*$^{-/-}$ cells (Figure 2B). Higher levels of c-Met and phospho–c-Met were also observed in murine *Pkd1*$^{-/-}$ E17.5 kidneys (Figure 2A). Increased expression of c-Met protein was confirmed in a second set of experiments in which *Pkd1* expression was knocked down in WT cells (KD4 cells [Supplemental Figure 1]; identical results were obtained with KD1 cells [data not shown]; supplemental material available online with this article; doi:10.1172/JCI41531DS1) (Figure 2D). c-Met protein levels were also elevated in protein extracts of human PKD kidneys (Figure 2C). Increased protein levels of c-Met could reflect either increased synthesis or defective degradation of the protein. No difference in *c-Met* mRNA levels was observed between *Pkd1*$^{+/+}$ and *Pkd1*$^{-/-}$ or *Pkd1*-knockdown cells (Figure 2, E and F). Translational control of c-Met expression has not yet been examined. However, a marked difference in post-stimulatory degradation of c-Met was observed: 30 minutes after HGF stimulation of serum-starved cells, the level of c-Met was reduced 6-fold in *Pkd1*$^{+/+}$ cells, but negligibly reduced in *Pkd1*$^{-/-}$ or *Pkd1*-knockdown cells (KD4) relative to the prestimulatory level of c-Met in each cell type (Figure 2, B and D). Finally, surface labeling of cells with membrane-impermeable biotin confirmed that most c-Met was localized to the plasma membrane in *Pkd1*$^{+/+}$ and *Pkd1*$^{-/-}$ or *Pkd1*-knockdown cells (Figure 3, A and B).

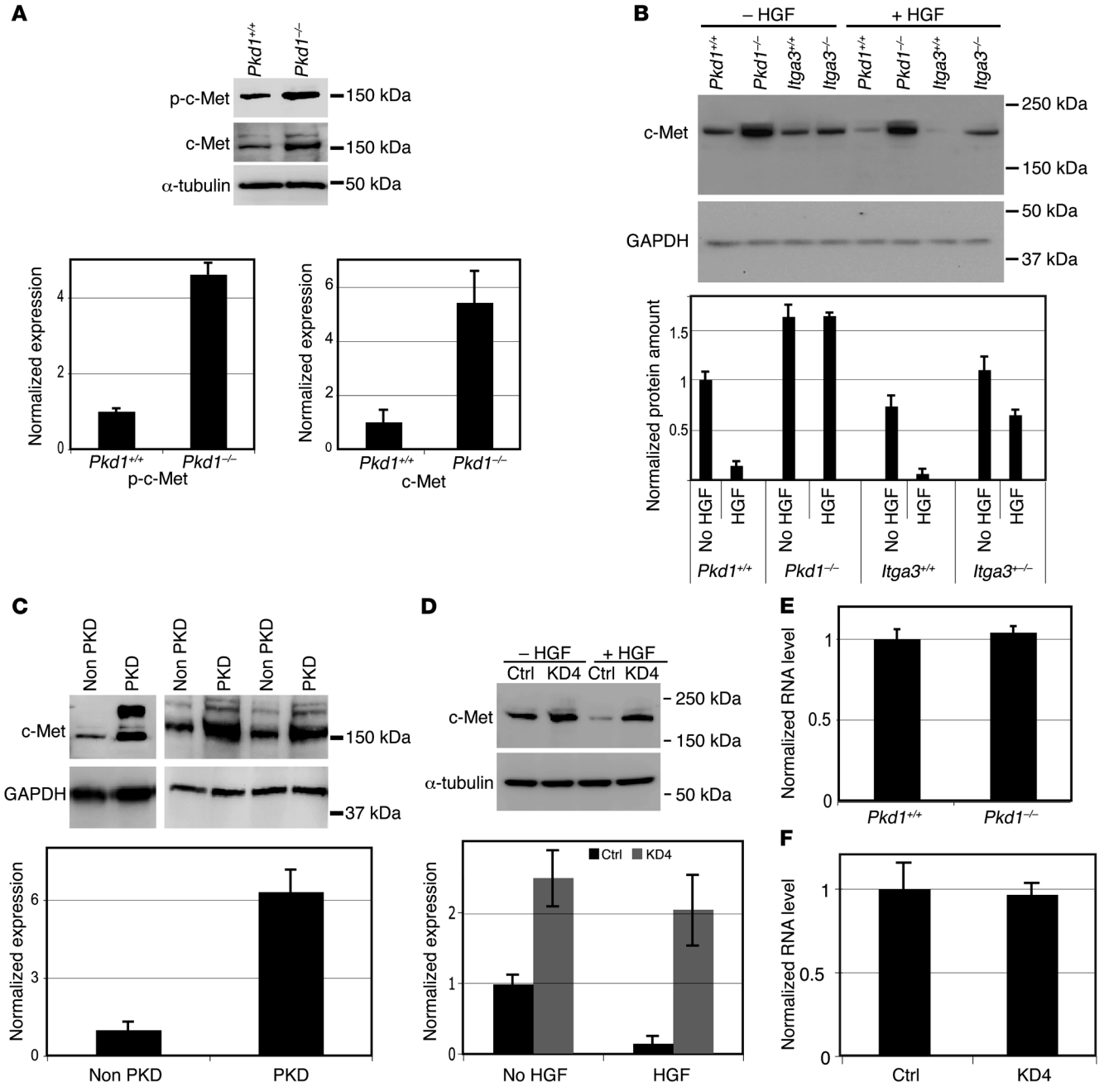

Figure 2

Increased expression and impaired degradation of c-Met in *Pkd1*$^{-/-}$ cells. (**A**) Western blot for phospho–c-Met (Tyr1234/1235) and c-Met in *Pkd1*$^{+/+}$ and *Pkd1*$^{-/-}$ E17.5 kidneys. Quantification is shown on the right. (**B**) Western blot of c-Met in *Pkd1*$^{+/+}$, *Pkd1*$^{-/-}$, *Itga3*$^{+/+}$, and *Itga3*$^{-/-}$ cells, with or without HGF stimulation (50 ng/ml HGF for 30 minutes). Densitometric quantification is shown on the right. c-Met was more abundant before stimulation and failed to be degraded in *Pkd1*$^{-/-}$ cells. Degradation was also reduced in *Itga3*$^{-/-}$ cells. GAPDH is shown as a loading control. (**C**) Western blot of c-Met in extract of human non-cystic and PKD kidneys. Higher levels of c-Met and an additional higher-molecular-weight species are present in the PKD sample. Densitometric quantification is shown on right, each bar represents the average of the 3 samples on left. (**D**) Western blot for c-Met after shRNA knockdown of *Pkd1* (KD4 cells), also showing increased levels of c-Met in nonstimulated cells and decreased degradation. (**E** and **F**) Reverse transcription quantitative PCR (RT-qPCR) for c-Met in *Pkd1*$^{+/+}$ and *Pkd1*$^{-/-}$ cells (**E**), or *Pkd1*$^{+/+}$ cells and KD4 cells (**F**). In **E** and **F**, the level of *c-Met* mRNA in *Pkd1*$^{-/-}$ cells is shown relative to the amount in *Pkd1*$^{+/+}$ or Ctrl cells. 18S RNA was used as an input control (**D**) and for normalization of RT-qPCR (**E** and **F**).

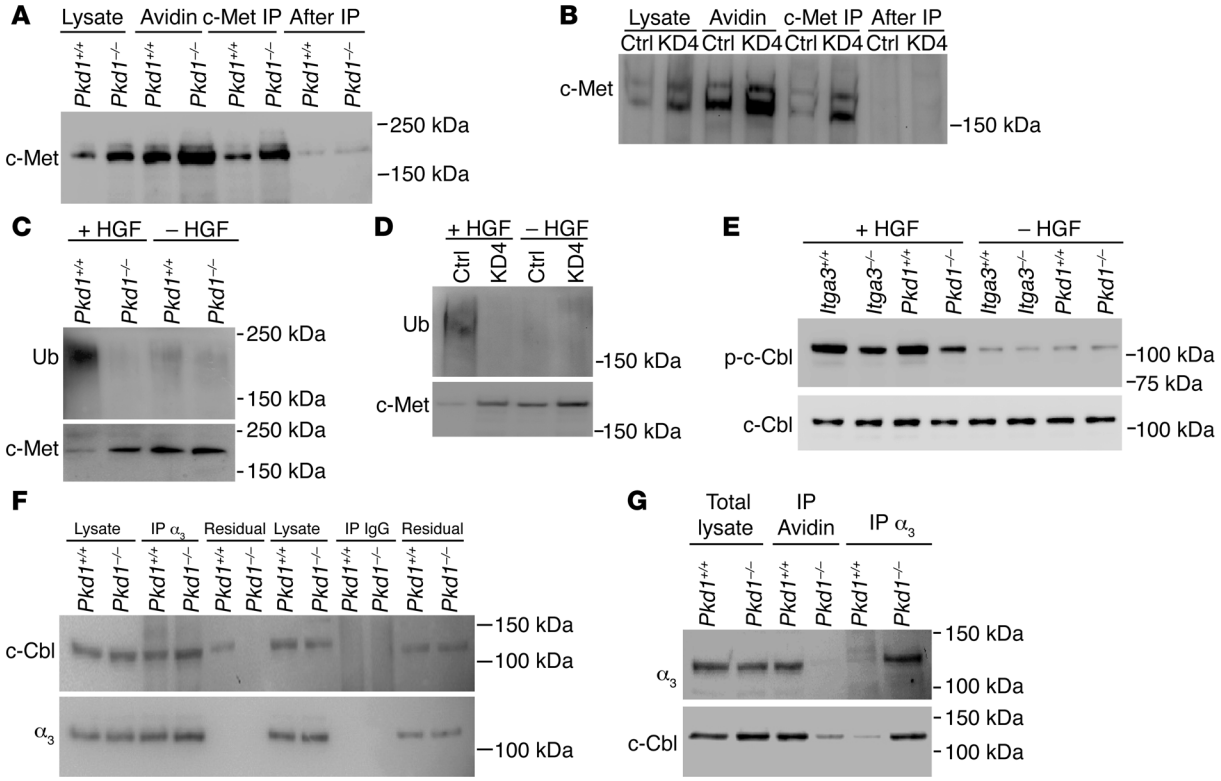

Figure 3

c-Met is localized at the plasma membrane in WT, *Pkd1*$^{-/-}$, and *Pkd1*-knockdown cells. Cells were labeled with membrane-impermeable sulfo-NHS-biotin; after extraction, labeled proteins were pulled down by avidin beads. Residual c-Met, representing unlabeled protein, was detected by c-Met immunoprecipitation. (**A** and **B**) Most c-Met is localized at the plasma membrane in WT, *Pkd1*$^{-/-}$, and KD4 cells. Little c-Met is detected in the post-immunoprecipitation fraction (after IP). (**C** and **D**) Failure to ubiquitinate c-Met in *Pkd1*$^{-/-}$ or KD4 cells. *Pkd1*$^{-/-}$ and *Pkd1*$^{+/+}$ cells (**C**) or KD4 and control cells (**D**) were stimulated with HGF, and cell lysates were immunoprecipitated with c-Met antibody and blotted with anti-ubiquitin. Nonstimulated cells showed little ubiquitination of c-Met. The immunoprecipitation was validated by a re-blot for c-Met (lower panels). (**E**) c-Cbl phosphorylation after HGF stimulation is decreased in *Pkd1*$^{-/-}$ cells. Control and mutant cells were incubated with HGF (50 ng/ml, 10 minutes). Phospho–c-Cbl and total c-Cbl were detected by Western blot. c-Cbl phosphorylation after HGF stimulation is weaker in both *Pkd1*$^{-/-}$ and *Itga3*$^{-/-}$ cells, compared with their WT controls. (**F**) c-Cbl binds $\alpha_3\beta_1$ integrin in both *Pkd1*$^{+/+}$ and *Pkd1*$^{-/-}$ cells. Pairs of lanes are designated as starting lysate, anti–α_3 integrin or non-immune IgG control immunoprecipitated material, and residual non-immunoprecipitated material. The membrane was reblotted with anti–α_3 integrin antibody to validate the immunoprecipitation. c-Cbl partially coimmunoprecipitated with $\alpha_3\beta_1$ integrin in *Pkd1*$^{+/+}$ and completely in *Pkd1*$^{-/-}$ cells. (**G**) $\alpha_3\beta_1$ integrin and c-Cbl are not localized to the membrane in *Pkd1*$^{-/-}$ cells. Cells were labeled with sulfo-NHS-biotin, labeled proteins were pulled down with avidin-coupled beads, and nonlabeled protein immunoprecipitated with anti–α_3 integrin. Western blots for α_3 integrin (upper panel) and c-Cbl (lower panel). In *Pkd1*$^{-/-}$ cells, little $\alpha_3\beta_1$ integrin or c-Cbl is localized at the plasma membrane.

Degradation of c-Met occurs through two distinct pathways. One pathway is ligand-dependent through ubiquitination; the other is ligand-independent through shedding of an extracellular domain (24, 25). Because difference in c-Met observed in our study reflected a post-stimulatory situation, we examined ubiquitination of c-Met. Abundant ubiquitination of c-Met after HGF stimulation was apparent in *Pkd1*$^{+/+}$ cells but virtually undetectable in *Pkd1*$^{-/-}$ cells (Figure 3C) or knockdown cells (Figure 3D). Addition of a proteasomal inhibitor (lactacystin) served to further demonstrate the failure to ubiquitinate c-Met in *Pkd1*$^{-/-}$ cells (Supplemental Figure 2). Ubiquitination of c-Met requires association of the c-Met cytoplasmic domain with c-Cbl, a c-Met E3 ubiquitin ligase, and subsequent phosphorylation of c-Cbl. Phosphorylation of c-Cbl after HGF stimulation was decreased in *Pkd1*$^{-/-}$ cells compared with *Pkd1*$^{+/+}$ cells (Figure 3E). Thus, the absence of polycystin-1 appeared to dramatically affect ubiquitination of c-Met through c-Cbl. c-Cbl is involved in the ubiquitination of other receptor tyrosine kinases, and similar deficient degradation was observed for EGFR and PDGFR-β (Supplemental Figure 3).

Sequestration of $\alpha_3\beta_1$ integrin and c-Cbl in the Golgi apparatus in Pkd1$^{-/-}$ *cells.* $\alpha_3\beta_1$ integrin is highly expressed by *Pkd1*$^{+/+}$ and *Pkd1*$^{-/-}$ cells. As c-Cbl is known to interact with integrins (26), the role of $\alpha_3\beta_1$ integrin in c-Cbl phosphorylation and localization was examined. Coimmunoprecipitation demonstrated abundant association of c-Cbl with $\alpha_3\beta_1$ integrin in *Pkd1*$^{+/+}$ cells; this association become nearly complete in *Pkd1*$^{-/-}$ cells, as little c-Cbl was found in residual extracts after immunodepletion with α_3 integrin antibody (Figure 3F). Additionally, biotinylation of cell surface proteins followed by affinity purification with immobilized NeutrAvidin protein beads confirmed the decreased membrane localization of $\alpha_3\beta_1$ integrin and c-Cbl in *Pkd1*$^{-/-}$ cells (Figure 3G). Furthermore, while costaining of $\alpha_3\beta_1$ integrin and c-Cbl in *Pkd1*$^{+/+}$ cells demonstrated membrane colocalization along cell-cell junctions (Figure 4A), both

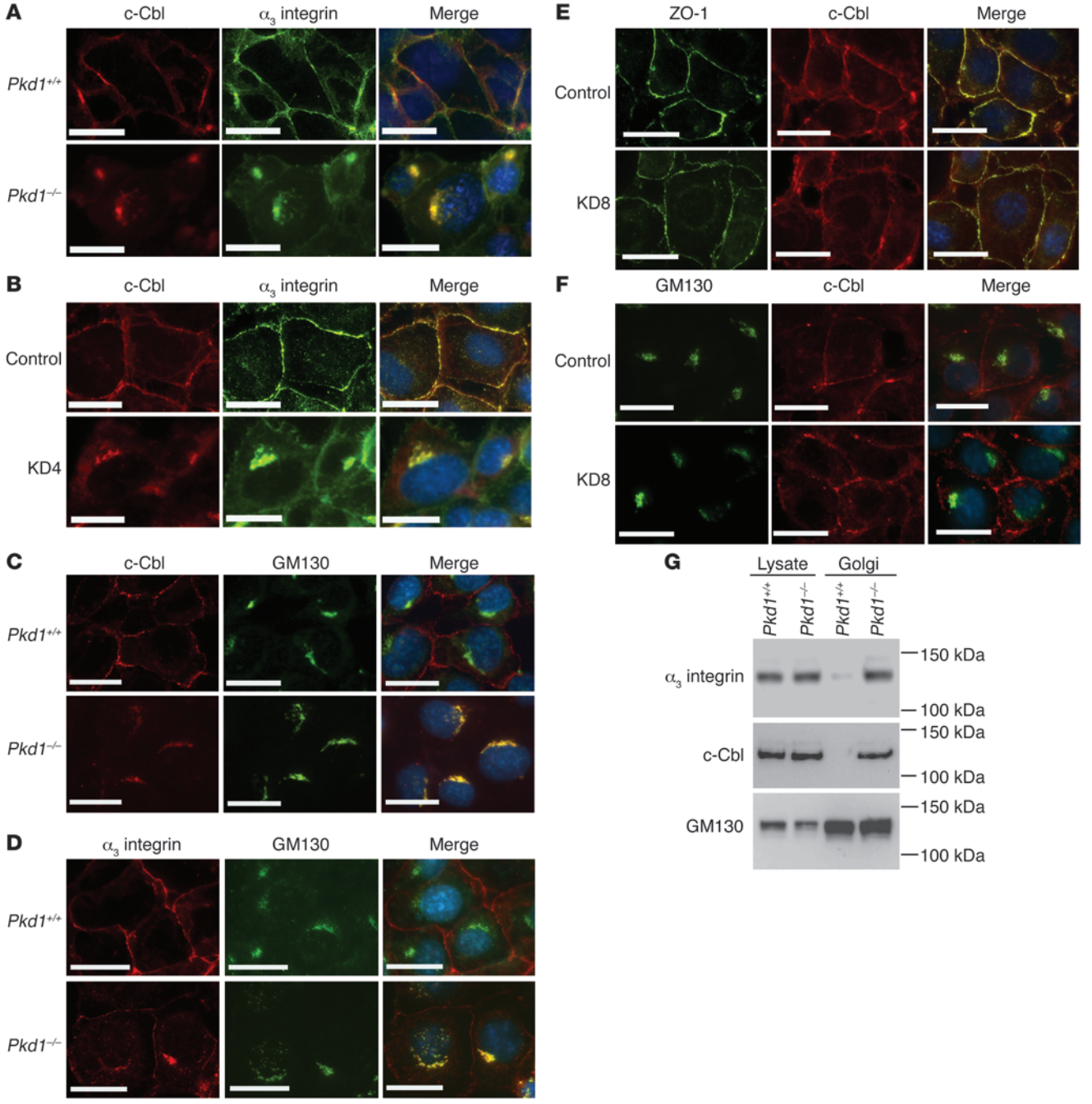

Figure 4

α_3 integrin and GM130 localization in *Pkd1*$^{+/+}$ and *Pkd1*$^{-/-}$ cells. (**A** and **B**) Colocalization of c-Cbl and $\alpha_3\beta_1$ integrin. Both c-Cbl and $\alpha_3\beta$ integrin are present in at cell-cell junctions in *Pkd1*$^{+/+}$ cells. In *Pkd1*$^{-/-}$ cells (**A**) or *Pkd1*-knockdown cells (KD4) (**B**), c-Cbl is concentrated in the perinuclear area, and $\alpha_3\beta_1$ integrin both is present at cell-cell junctions and colocalizes with c-Cbl in a perinuclear pattern. (**C**) c-Cbl and (**D**) $\alpha_3\beta_1$ integrin colocalize (yellow staining) with GM130, a Golgi marker, in *Pkd1*$^{-/-}$ but not *Pkd1*$^{+/+}$ cells. (**E**) In *Itga3*$^{-/-}$ *Pkd1*-knockdown (KD8) cells, c-Cbl is localized at the plasma membrane, as demonstrated by overlapping staining with ZO-1. (**F**) c-Cbl does not colocalize with GM130 in KD8 cells. Scale bars: 20 μm. (**G**) Discontinuous sucrose gradient enrichment of the Golgi apparatus from *Pkd1*$^{+/+}$ and *Pkd1*$^{-/-}$ cells. Both $\alpha_3\beta_1$ integrin and c-Cbl are present in the Golgi-enriched fraction from *Pkd1*$^{-/-}$ cells, but neither was detected in the Golgi-enriched fraction from *Pkd1*$^{+/+}$ cells. The Western blot of GM130 in the lower panel validates the Golgi enrichment.

$\alpha_3\beta_1$ integrin and c-Cbl acquired a predominantly cytoplasmic localization in *Pkd1*$^{-/-}$ or *Pkd1*-knockdown KD4 cells (Figure 4, A and B). The appearance of $\alpha_3\beta_1$ integrin and c-Cbl staining was suggestive of localization within the Golgi apparatus; this was confirmed by costaining with the Golgi marker GM130, which only overlapped with c-Cbl and $\alpha_3\beta_1$ integrin in *Pkd1*$^{-/-}$ cells (Figure 4, C and D), but not in *Pkd1*$^{+/+}$ cells. To determine whether $\alpha_3\beta_1$ integrin was indeed required for the sequestration of c-Cbl

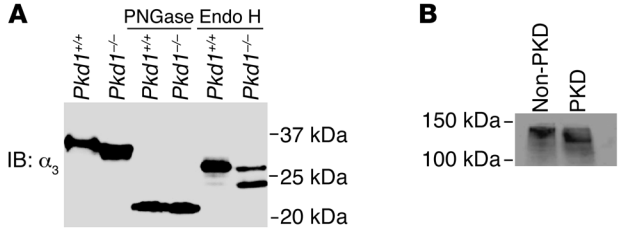

Figure 5

Defective glycosylation of α_3 integrin. (**A**) Defective glycosylation of α_3 integrin subunit in *Pkd1*$^{-/-}$ cells. Western blot using an α_3 integrin antibody. Treatment with Endo H or PNGase is designated above the lanes; the first two lanes are untreated. PNGase removes all N-linked glycosylation, whereas Endo H removes only high mannose glycosylation. α_3 Integrin subunit shows a faster migration in *Pkd1*$^{-/-}$ cells than *Pkd1*$^{+/+}$ cells. Digestion with deglycosylating enzymes eliminates this difference. (**B**) Western blot of α_3 integrin in samples of human PKD and non-cystic kidneys. Faster migration is observed in the sample from a PKD kidney. The GAPDH loading control for this blot is that shown in Figure 2C. **A** is from a reducing gel blotted with α_3 integrin C-terminal antibody, and **B** is from a nonreducing gel blotted with α_3 integrin N-terminal antibody.

in *Pkd1*$^{-/-}$ cells, we knocked down *Pkd1* in *Itga3*$^{-/-}$ cells (KD8 cells, Supplemental Figure 1). In the absence of $\alpha_3\beta_1$ integrin, c-Cbl was no longer sequestered in the Golgi in *Pkd1*-knockdown cells and was able to localize to the plasma membrane, as demonstrated by costaining with the junctional protein ZO-1 (Figure 4, E and F). When discontinuous sucrose gradient separation was used to enrich a Golgi apparatus fraction, $\alpha_3\beta_1$ integrin and c-Cbl were found in the Golgi apparatus-enriched fraction of *Pkd1*$^{-/-}$ cells but not *Pkd1*$^{+/+}$ cells (Figure 4G).

We have recently demonstrated (27) that $\alpha_3\beta_1$ integrin is required for c-Met to be activated following stimulation by HGF, raising the question of how activation of c-Met may be involved in cystogenesis if $\alpha_3\beta_1$ integrin is sequestered in the Golgi. However, a small fraction of α_3 integrin remained localized in the plasma membrane in *Pkd1*$^{-/-}$ cells (Figure 4A) and, more obviously, in *Pkd1*-knockdown cells (Figure 4B), which may have accounted for the ability of c-Met to be activated in *Pkd1*$^{-/-}$ cells. Moreover, in contrast to the abnormal localization of $\alpha_3\beta_1$ integrin and c-Cbl, surface labeling with membrane-impermeable biotin reagent demonstrated that c-Met was mainly localized to the cell membrane in WT, *Pkd1*$^{-/-}$, and *Pkd1*-knockdown (KD4) cells (Figure 3, A and B).

The association of c-Cbl with $\alpha_3\beta_1$ integrin prompted us to examine a possible requirement for $\alpha_3\beta_1$ integrin in the c-Cbl–mediated degradation of c-Met. Equivalent amounts of c-Met (Figure 2B) and c-Cbl (Figure 3E) were present in *Itga3*$^{+/+}$ and *Itga3*$^{-/-}$ cells (28). Furthermore, c-Cbl was localized at the plasma membrane in *Itga3*$^{-/-}$ cells (Supplemental Figure 3). However, c-Cbl phosphorylation after HGF stimulation was decreased in *Itga3*$^{-/-}$ cells (Figure 3E), and as in *Pkd1*$^{-/-}$ cells after HGF stimulation, c-Met was incompletely degraded in *Itga3*$^{-/-}$ cells (Figure 2B). Thus, $\alpha_3\beta_1$ integrin has a role, though not absolute, in obtaining maximal degradation of c-Met. Most likely, this relates to the requirement for $\alpha_3\beta_1$ integrin to maximally activate c-Met– and c-Cbl–mediated degradation.

Together, these results suggest that the abnormal accumulation of c-Met in *Pkd1*$^{-/-}$ cells may result from the decreased activation of c-Cbl and deficient ubiquitination of c-Met. The resultant effect of this abnormal handling of c-Met appears to be the hyperactivation of mTOR.

Glycosylation of $\alpha_3\beta_1$ integrin subunit is defective in Pkd1$^{-/-}$ *cells.* The finding that $\alpha_3\beta_1$ integrin and c-Cbl were mislocalized in the Golgi in *Pkd1*$^{-/-}$ cells was reminiscent of findings that E-cadherin was also improperly processed in the Golgi apparatus in *Pkd1* mutant cells (29). Since the modification of protein glycosylation is a major event occurring in the late endoplasmic reticulum and Golgi, the glycosylation of the α_3 subunit was examined. We observed that the α_3 integrin subunit displayed abnormal mobility in SDS-PAGE electrophoresis (Figure 5A). Moreover, treatment of the cell lysate with alkaline phosphatase did not eliminate this difference in mobility (data not shown), which argues against the possibility of differential protein phosphorylation between *Pkd1*$^{+/+}$ and *Pkd1*$^{-/-}$ cells. In contrast, treatment with PNGase F eliminated the difference in mobility (Figure 5A), and comparison of the migration after treatment with PNGase F versus Endo H indicated that a greater proportion of the α_3 subunit was processed to an Endo H–resistant form, while a greater proportion retained greater Endo H sensitivity in *Pkd1*$^{-/-}$ cells. These results are more consistent with defects in glycosylation occurring in the late endoplasmic reticulum or Golgi apparatus that are responsible for removing the high mannose structure and conferring complex glycosylation patterns on glycoproteins. A similar change in migration of the α_3 integrin subunit in electrophoresis was also observed in an extract of a kidney from a human individual with PKD (Figure 5B).

Altered distribution of c-Cbl and $\alpha_3\beta_1$ integrin in vivo in Pkd1$^{-/-}$ *kidneys.* To confirm that our findings with immortalized cell lines were relevant to changes that occurred in vivo, we compared the localization of $\alpha_3\beta_1$ integrin and c-Cbl in epithelial cells of *Pkd1*$^{+/+}$ and *Pkd1*$^{-/-}$ kidneys. As predicted, both $\alpha_3\beta_1$ integrin and c-Cbl showed a basolateral distribution in tubules of WT kidneys (Figure 6, A and B). In contrast, and reflecting the in vitro observations, in epithelial cells lining the cysts of *Pkd1*$^{-/-}$ kidneys, both c-Cbl and $\alpha_3\beta_1$ integrin localized in a perinuclear distribution (Figure 6, A and B). Similar findings were obtained using specimens from a PKD human individual (Figure 6C). These in vivo data confirmed that c-Cbl and $\alpha_3\beta_1$ integrin are sequestered in the cytoplasm of epithelial cells and cannot be correctly targeted to the plasma membrane.

Treatment of Pkd1$^{-/-}$ *cystic kidneys in organ culture with c-Met inhibitor can decrease the size and number of kidney cysts.* These observations predict that blockade of signaling by c-Met would reduce cyst formation in *Pkd1*$^{-/-}$ kidneys. As a first test of this hypothesis, embryonic organ cultures from WT and *Pkd1*$^{-/-}$ kidneys were treated with a pharmacological blocker of c-Met (Su11274, Calbiochem, used at 5 μM). Typically, kidneys placed in organ culture, even from *Pkd1*$^{-/-}$ mice, do not develop or maintain cysts unless treated with 8-Br-cAMP (30), a membrane-permeable cAMP analog that is more resistant to phosphodiesterase cleavage than cAMP and that preferentially activates cAMP-dependent protein kinase (PKA) (31, 32). An appropriate concentration of 8-Br-cAMP was titrated to promote prominent cyst formation in *Pkd1*$^{-/-}$ kidneys but little in WT kidneys. Treatment with the c-Met inhibitor reduced cyst formation in organ culture in *Pkd1*$^{-/-}$ mutant kidneys to the minimal level observed in WT kidneys (Figure 7A). Similar results were obtained with a second c-Met inhibitor (PHA665752, Tocris, used at 0.5 μM) or a c-Met blocking antibody (R&D Systems, used at 5 μg/ml) (data not shown). Importantly, the c-Met inhibitor did not have a marked effect on nephrogenesis in either WT or mutant kidneys (Supplemental Figure 2).

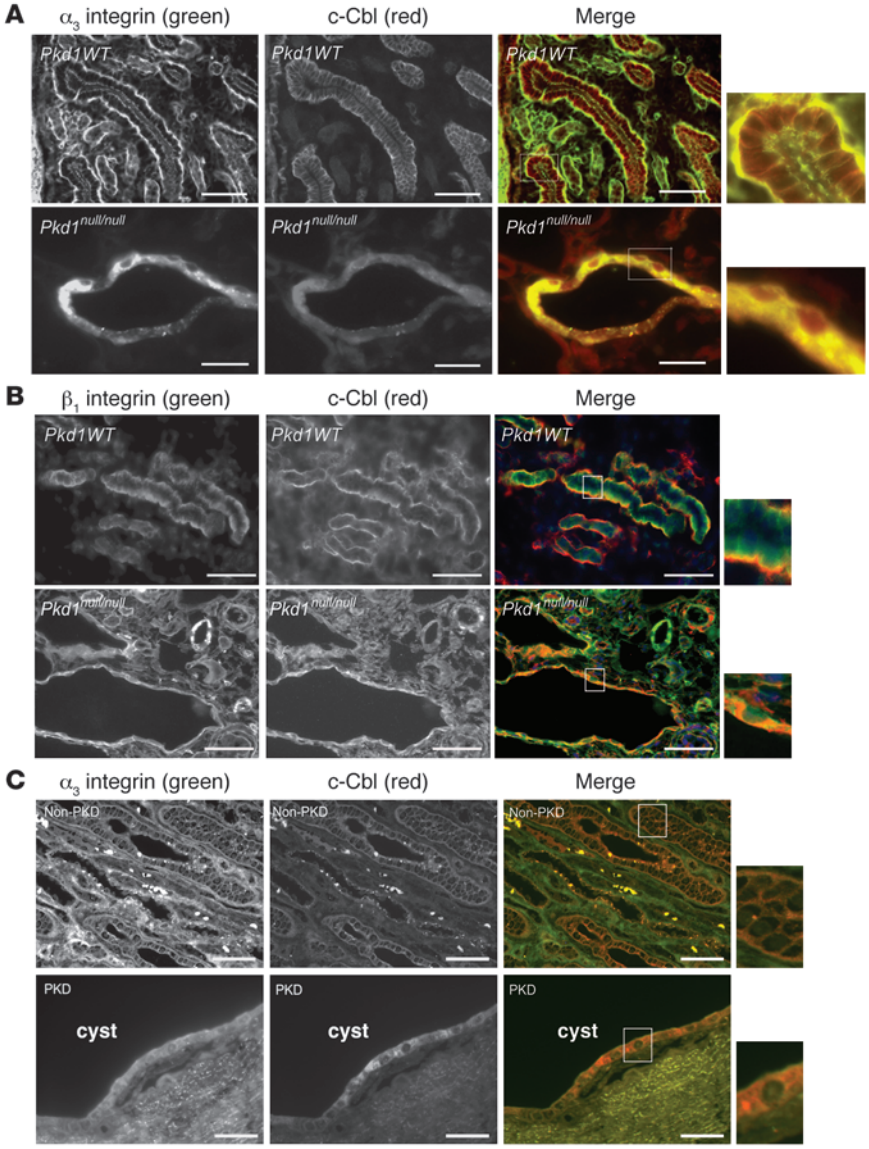

Figure 6
Inhibition of Akt and S6K activity in vivo by c-Met inhibitor. Differential localization in vivo for $\alpha_3\beta_1$ integrin and c-Cbl in WT and *Pkd1*$^{-/-}$ mouse kidneys. (**A**) Costaining for α_3 integrin and c-Cbl. (**B**) Costaining for β_1 integrin and c-Cbl. In each panel, the genotype is noted in the upper-left corner, and the stain is noted above. The third panel in each row shows an overlay, with a magnified image (×600) in the fourth panel. $\alpha_3\beta_1$ integrin is present in a basolateral distribution in WT and a cytoplasmic distribution in the *Pkd1*$^{-/-}$ tubules. c-Cbl has a basal distribution in WT and cytoplasmic localization that overlaps with $\alpha_3\beta_1$ integrin in *Pkd1*$^{-/-}$ tubules. (**C**) Staining for c-Cbl and $\alpha_3\beta_1$ integrin in human non-cystic and PKD kidneys, showing basolateral localization of c-Cbl and $\alpha_3\beta_1$ integrin in the non-PKD sample and perinuclear pattern in the PKD sample. Scale bars: 50 μm.

Based on the results with organ cultures, the c-Met inhibitor was then used to treat pregnant mice carrying litters that included *Pkd1*$^{-/-}$ embryos, which normally develop dramatic cysts by E18. Pregnant females were treated twice daily between E14 and E17, and embryonic kidneys were examined at E18.5. There was a marked reduction in cyst numbers and size in kidneys of *Pkd1*$^{-/-}$ embryos in treated versus control litters (the total cyst area reduced from approximately 47% to 19%, $P = 0.003$) (Figure 7, B and D). Examination of WT kidneys from treated litters revealed no adverse effects on nephrogenesis (Figure 7C). To elucidate whether c-Met inhibitor treatment can inhibit Akt/mTOR signaling in our system, we examined phosphorylation status of Akt and S6K, one of the mTOR substrates, after treatment with c-Met inhibitor or vehicle. Compared with vehicle, the c-Met inhibitor decreased activation of Akt and S6K (Figure 8).

Discussion

Despite the significant morbidity associated with autosomal dominant PKD (ADPKD), there are no approved treatments specifically targeted toward molecular pathways that are aberrantly regulated in this relatively common hereditary disease. Here we suggest that c-Met might be a therapeutic target in PKD. In the present study, we have shown that in *Pkd1*$^{-/-}$ cells, there is a hyperactivation of c-Met signaling, due to a failure to ubiquitinate c-Met following stimulation with HGF. A role for HGF signaling in cystic disease was suggested by previous studies in which transgenic mice overexpressing HGF developed prominent tubular cysts in their kidneys (33) and elevated levels of HGF have been detected in cyst fluid from PKD patients (6). Normally, activation of c-Met leads to recruitment and phosphorylation of c-Cbl, an E3 ubiquitin ligase for c-Met. Defective ubiquitination of c-Met in *Pkd1*$^{-/-}$ cells appears to be due to sequestration of c-Cbl in the Golgi apparatus by $\alpha_3\beta_1$ integrin. Hyperactivated c-Met signaling results in increased mTOR activity in *Pkd1*$^{-/-}$ cells. As a validation of the role of c-Met in the formation of cysts in ADPKD, a c-Met inhibitor was shown to inhibit cyst formation in an ex vivo organ culture model of ADPKD, and also in embryonic *Pkd1*$^{-/-}$ kidneys through inhibition of Akt and S6K phosphorylation. These find-

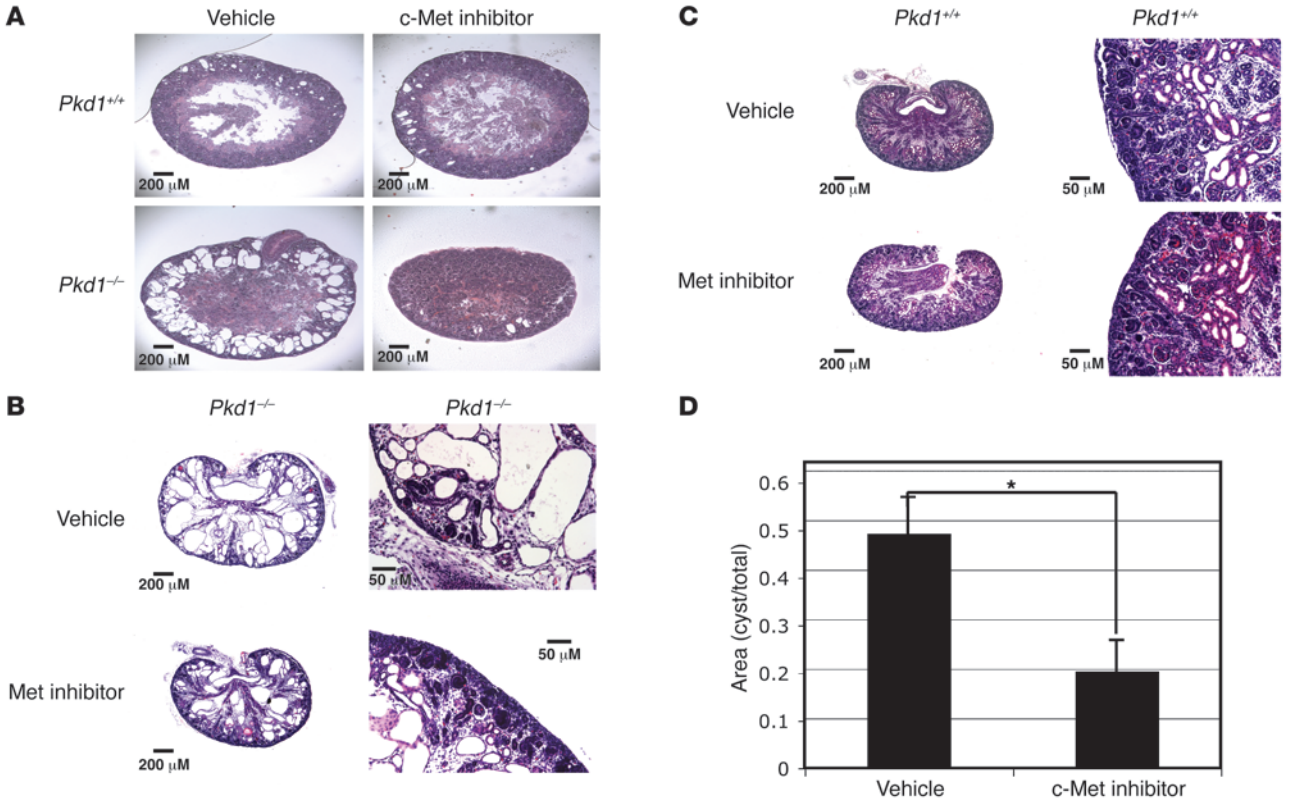

Figure 7

A c-Met inhibitor decreased the size and number of cysts in *Pkd1*$^{-/-}$ kidneys. (**A**) Treatment in an organ culture model of PKD. The genotype and treatment are noted on the left and above the panels, respectively. *Pkd1*$^{+/+}$ and *Pkd1*$^{-/-}$ mice kidneys at E15.5 were removed from embryonic mice and put in organ culture dishes, containing media with 10 μM 8-Br-cAMP. Twelve hours later, either 5 μM c-Met inhibitor Su11274 (dissolved in DMSO) or the same amount of DMSO was added to the media. Hematoxylin and eosin–stained sections of kidneys are shown after 96 hours of treatment. Scale bars: 200 μm. (**B**) Treatment of pregnant mice with c-Met inhibitor. *Pkd1*$^{+/-}$ pregnant mice that had been mated with *Pkd1*$^{+/-}$ male mice were treated twice daily between E14 and E17 with vehicle only (top row) or c-Met inhibitor (bottom row). c-Met inhibitor treatment can decrease cyst formation in *Pkd1*$^{-/-}$ embryonic kidneys. A high-power view is shown at right. (**C**) Kidney development in utero in WT kidneys was not affected by treatment with c-Met inhibitor. Top panels: WT kidney from vehicle-only treatment; bottom panels: WT kidney from c-Met inhibitor–treated litter. Scale bars in **B** and **C**: 200 μm (left), 50 μm (right). (**D**) Quantitative analysis of cystic area in *Pkd1*$^{-/-}$ embryonic kidneys treated with vehicle or c-Met inhibitor. Kidneys from 9 pairs of vehicle and c-Met inhibitor–treated mice were quantified by NIS-Elements BR. The difference in cyst area between vehicle- and c-Met inhibitor–treated group is significant (*P = 0.003), as analyzed by paired Student's t test.

ings suggest that hyperactivated c-Met signaling may be causative for mTOR activation and c-Met inhibitors may represent a new strategy to treat PKD.

c-Met and hyperactivation of mTOR. Epithelial cells lining cysts of ADPKD kidneys exhibit high mTOR activity (22). Rapamycin, an mTOR inhibitor, has been shown to be effective in alleviating the cystic phenotype in the *Tg737*$^{orpk/orpk}$ mouse model for PKD (22). Furthermore, in individuals with PKD, rapamycin treatment for immunosuppression after kidney transplantation reduces the volume of cysts in the recipients' native kidneys (22). One hypothesized role of mTOR in PKD relates to its negative regulation by tuberin, the product of the *TSC2* gene, known to be mutated in tuberous sclerosis. Tuberin is itself negatively regulated by PI3K/Akt. Polycystin-1, the product of the *Pkd1* gene, is also known to associate with tuberin, providing a possible mechanistic link between the loss of polycystin-1 expression and hyperactivation of mTOR. Our results provide an additional mechanistic explanation for the hyperactivation of mTOR, suggesting that it occurs downstream of c-Met. The two major processes thought to contribute to cystogenesis are increased proliferation and fluid secretion (34–36). A role for proliferation in PKD is supported by findings of increased BrdU incorporation (37), Ki-67 staining (38), and PCNA staining (39) in cyst-lining cells. Hyperactivation of c-Met would likely lead to increased proliferation (40, 41), consistent with these findings. On the other hand, Piontek et al. failed to find an increase in proliferation, and thus, the role of proliferation in PKD remains controversial (42). Whether signaling through c-Met could affect fluid secretion and other cell behaviors that might convert epithelial cells to a cystic phenotype remains to be determined.

Golgi defects in PKD. Our proposed mechanism for mTOR overactivation — that is, defective ubiquitination of c-Met secondary to sequestration of c-Cbl in the Golgi — raises the question of why the absence of polycystin-1 may affect protein modification and transport within the Golgi apparatus. Other reports have also identified abnormal Golgi function in PKD, including abnormal proteoglycan synthesis and altered intracellular transport of proteoglycan in ADPKD (43–46). Impaired basolateral trafficking of proteins and lipids, including E-cadherin and C6-NBD-ceramide, has been

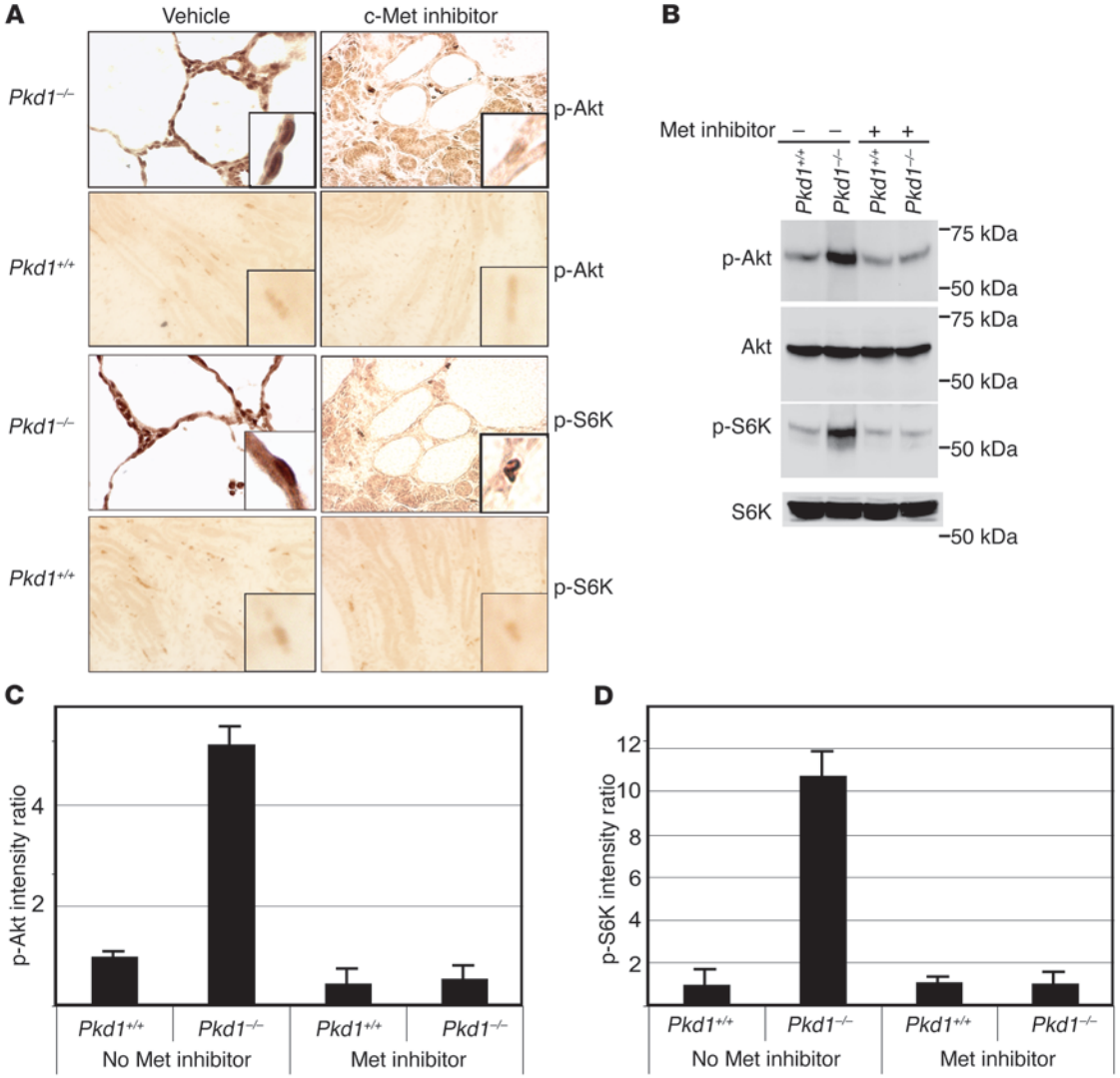

Figure 8

Inhibition of Akt and S6K activity in vivo by c-Met inhibitor. Immunohistochemical staining (**A**) and Western blot analysis (**B**) of phospho-Akt and phospho-S6K in vehicle- and c-Met inhibitor–treated embryonic kidneys. Genotypes are indicated at left and treatment above each column. Each inset in **A** shows a higher-power view (×600). c-Met inhibitor treatment decreases staining of phosphorylated Akt and phosphorylated S6K in *Pkd1*$^{-/-}$ embryonic kidneys. Scale bars: 50 μm. (**B**) Western blot for phospho-Akt and phospho-S6K in kidneys of c-Met inhibitor–treated and untreated embryos. Re-blots for total Akt and total S6K are shown below the anti–phospho-protein blots. (**C**) Quantification of phospho-Akt staining. (**D**) Quantification of phospho-S6K staining.

reported in ADPKD cells as a result of defective cargo exit from the Golgi (29, 47). Impaired trafficking of sulfated glycoproteins has also been reported in ADPKD (48). The aberrant glycosylation of the α_3 integrin subunit may represent a primary defect leading to abnormal transport through the Golgi apparatus or may be secondary to another defect in protein transport. However, since c-Cbl is not a glycosylated protein, it is unlikely that a transport defect relating to glycosylation would affect c-Cbl similarly to glycosylated proteins such as $\alpha_3\beta_1$ integrin or E-cadherin. Additionally, the Golgi apparatus were flattened and deformed in *Pkd1*$^{-/-}$ cells, which serves as an additional indication of a major Golgi defect in PKD (47). Finally, a recent report showed that in polycystin-2–depleted *Schizosaccharomyces pombe*, plasma membrane proteins are also trapped in the Golgi apparatus (49). Together, these observations suggest a major, though not complete, defect of protein processing in the Golgi and protein trafficking in ADPKD. Defective trafficking in PKD may relate to mislocalization of Rab proteins; for example, Rab8 was previously shown to be mislocalized from the Golgi in ADPKD cells (47).

Receptor tyrosine kinases signaling in PKD. The c-Met inhibitor was able to effectively block activation of mTOR in *Pkd1*$^{-/-}$ cells. However, we also demonstrated deficient degradation of other receptor tyrosine kinases, including EGFR and PDGRFβ. This raises the question of whether c-Met is the only receptor tyrosine kinase involved in cyst formation. This is an important question, because if cyst formation results from increased expression of multiple receptor tyrosine kinases, this provides an avenue for combination therapies that involve subtoxic doses of multiple agents, rather

than higher doses of a single agent, to prevent cyst formation in individuals with PKD. It is well established that there is considerable crosstalk between different receptor tyrosine kinases; this is especially well studied for c-Met and EGFR (50). Thus, it is possible that addition of the c-Met inhibitor, while primarily affecting c-Met, may also indirectly affect activation of EGFR and other receptor tyrosine kinases.

c-Met and epithelial morphogenesis. c-Met has received intense study for its role in epithelial morphogenesis. The ability of HGF to induce the formation of branched tubules in 3D collagen gels has suggested a role for c-Met signaling in branching morphogenesis. A potential model for branch formation suggests that branches are initiated when epithelial cells fail to restrict the orientation of cell division to a 2D monolayer or to the long axis of a simple tubule and instead orient the axis of cell division such that cells emerge from the tubule to initiate a branching event. The regulatory events that govern the orientation of cell division are thought to be a manifestation of planar cell polarity (PCP), a term used to describe how cell behavior is regulated by cellular interactions between lateral membranes (as opposed, for instance, to processes that regulate apical-basal polarity) to govern cell behavior within a plane. One major way in which PCP-related processes may regulate cell behavior is by regulating the orientation of mitotic spindles during cell division. Whether abnormal regulation of PCP has a role in cyst disease is presently undergoing important consideration (51). There are now several examples of randomized or inappropriate mitotic spindle orientation in various models of PKD, including the PCK rat model of cystic disease (52), FAT4 mutant mice (53), and Kif3a conditional mutant mice (54).

A possible role for c-Met in regulating PCP is suggested by several observations. First, signaling downstream of c-Met, as with other receptor tyrosine kinases, has the capacity to disrupt cell-cell interactions, in part by causing increased tyrosine phosphorylation of β-catenin (55) and consequent disruption of cadherin-mediated cell-cell adhesion, facilitating the exit of cells from a monolayer or the initiation of a branch point. Second, it has been observed that HGF stimulation can result in increased variation in mitotic spindle orientation (56) that would also facilitate the initiation of a branch point in a simple tubule. Taken together, these observations suggested an association between aberrant HGF/c-Met signaling and cystogenesis in the kidney. How might these normal functions of c-Met in epithelial morphogenesis be co-opted to result in cyst formation in PKD? Hyperactivation of c-Met may contribute to excessive randomization of mitotic spindle orientation, as has been shown to occur in cystic disease (52), replacing branching events with the initiation of cysts. It may also contribute by excessive disruption of cadherin mediate cell-cell adhesion, contributing to the abnormal morphology of cyst-lining cells that are highly flattened along the basement membrane, with minimal lateral junctions.

Golgi function and cilia in PKD. Cilia are the present focal point of research on PKD (57). Polycystins-1 and -2 and many other proteins involved in cystogenesis are localized to the cilia, among other subcellular compartments (58). Several recent observations have begun to draw physical links between the cilia and the Golgi apparatus (47, 59). For example, several proteins including IFT20, dyenin2, and kinesin-2 are found in both the Golgi apparatus and cilia (60). It is suggested that IFT20 functions in the delivery of ciliary membrane proteins from Golgi complex to the cilium. Furthermore, there may be structural continuity between Golgi and the centrosome as well as basal body of the primary cilia (61, 62). These observations suggest that a primary Golgi defect may lead to cilia malfunction and cyst formation in PKD.

On the other hand, it is more difficult to formulate hypotheses about how a primary cilia defect might cause abnormal protein processing in the Golgi. One possibility is that this is very indirect and results from abnormal regulation of gene expression by signals transduced from the cilia. For example, the cilia is a major locus of sonic hedgehog signaling, and the abnormal ratios of Gli activator to repressor isoforms that might be expected to result from ciliary dysfunction could be predicted to have important effects on gene expression, including of genes that encode proteins involved in protein trafficking, as this constitutes a large group of proteins within the cell.

Methods

Reagents. Antibodies included rabbit polyclonal anti–mouse α_3 integrin (custom prepared by Invitrogen), goat polyclonal α_3 integrin (Santa Cruz Biotechnology Inc. N-19), rabbit polyclonal anti–mouse mTOR, and anti–mouse phospho-mTOR (Cell Signaling Technology 2972 and 2971), mouse monoclonal anti–mouse c-Met (Cell Signaling Technology 3127), c-Met blocking antibody (R&D Systems AF527), mouse monoclonal anti–mouse ubiquitin (Cell Signaling Technology 3936), rabbit polyclonal anti–mouse c-Cbl (Santa Cruz Biotechnology Inc. sc-170), mouse monoclonal anti–mouse GM130 (BD 610822). c-Met inhibitor Su11274 was purchased from Calbiochem and PHA665752 from Tocris. EZ-Link Sulfo-NHS-Biotin was purchased from Thermo Fisher Scientific (catalog 21217). Hepatocyte growth factor was obtained from Sigma-Aldrich (catalog H1404). Unless otherwise stated, all other chemicals were purchased from Sigma-Aldrich.

Human PKD samples. Anonymous human PKD samples were provided by Helmut Rennke (Brigham and Women's Hospital) and used with approval of the Partners Human Research Committee, Boston, Massachusetts, USA.

Cells and mice. *Pkd1*$^{-/-}$ mice were previously described (23). *Pkd1*$^{+/+}$ and *Pkd1*$^{-/-}$ cell lines (23) (used at passages 9–14) and *Itga3*$^{+/+}$ and *Itga3*$^{-/-}$ cell lines (28, 63) (used at passage 6–14) were previously described. All cells were cultured in DMEM containing 2% fetal bovine serum, 0.75 μg/l γ-interferon, 1.0 g/l insulin, 0.67 mg/l sodium selenite, 0.55 g/l transferrin, 36 ng/ ml hydrocortisone, 100 U/ml penicillin/streptomycin under 33°C and 5% CO_2 (64).

Lentiviral preparation, viral infection, and stable cell line generation. The lentiviral hairpin-pLKO.1 vector encoding target sequence was transfected into HEK293T cells along with pCMV-dR8.91 and VSV-G/pMD2G using TransIT-LT1, and viruses were collected from media at approximately 40 hours after transfection. Target cells grown on 6-cm dishes were infected with viruses in the presence of polybrene. Individual cell colonies were selected and isolated in the presence of puromycin at a concentration of 2.4 μg/ml. Stable cell lines were maintained in the media containing 2 μg/ml puromycin. Knockdown efficiency was analyzed by quantitative PCR and Western blot. The target sequence of the constructs were KD1: CGCTCGCACTTTCAGCAATAA; KD2: GCCCTGTACCTTTCAACCAAT; KD3: CCAACTCAACATCACCGTAAA; KD4: GCTTCACTACTCTTCCTGCTT. The primers used for Pkd1 amplification in quantitative PCR were forward primer: TCTCGGAGCAGAATCAATGCC; reverse primer: CAGAGTTGAGGGACAGTGAGAT. The control construct for knockdown experiments was a pLKO.1 empty lentiviral vector that did not contain an shRNA insert; cells derived with this vector are referred to as "Ctrl" in the figures.

Immunoprecipitation and Western blot. Immunoprecipitation and Western-blot analysis were performed using whole cell lysates unless otherwise specified. Confluent cells were collected, washed with PBS, lysed with lysis buffer (20 mM Tris/HCl, 1 mM EDTA, 150 mM NaCl, 1% Triton X-100) containing proteinase inhibitor cocktail tablet (Roche 1697498) at 4°C for 30 minutes. After centrifugation at 15,700 *g* for 15 minutes, supernatants

were incubated with specific antibody at 4°C for 1 hour, followed by incubation with Protein G–conjugated beads (Pierce Biotechnology) at 4°C for 2 hours, and then samples were washed in lysis buffer. Samples were run on 7.5% acrylamide gel and transferred to PVDF membranes, followed by immunoblotting with specified antibodies.

Immunofluorescence. Cultured cells or cryosections (embedded in OCT and cut in a thickness of 5 μm) were fixed in cold methanol at –20°C for 10 minutes, blocked in 2% BSA for 1 hour, and incubated overnight at 4°C with primary antibody and then with Alex Fluor 488– or Alex Fluor 594–labeled secondary antibody at room temperature for 1 hour. Images were taken with the same exposure time for the same antibody.

Immunohistochemistry. Paraffin sections (5 μM) of 4% paraformaldehyde–fixed kidneys were placed in citrate-buffered solution (pH 6.0) and then boiled for 30 minutes for antigen retrieval. Endogenous peroxidase was blocked with 3% hydrogen peroxide, and nonspecific binding was blocked with 10% BSA. Diaminobenzidine substrate (Sigma-Aldrich) was used for the color reaction. Secondary antibody alone was consistently negative on all sections.

mTOR phosphorylation and activation. *Pkd1*$^{-/-}$ and WT cells were treated with either HGF (Sigma-Aldrich, 50 ng/ml, 20 minutes) or Met Kinase Inhibitor (Calbiochem, 5 μM, 4 hours). Blotting with phospho-mTOR antibody, phospho-S6K, total mTOR, or total S6K antibody was used to analyze mTOR phosphorylation and activation.

c-Met degradation. WT and *Pkd1*$^{-/-}$ cells were stimulated with 50 ng/ml HGF for 30 minutes, lysed, and subjected to Western blot analysis to determine the c-Met amount, normalized to GAPDH. Band density was measured by densitometry (Gel Doc XR, Bio-Rad), according to the manufacturer's instructions.

Sequential precipitation with avidin and α_3 integrin antibody. Confluent WT and *Pkd1*$^{-/-}$ cells were labeled with membrane-impermeable EZ-Link Sulfo-NHS-Biotin. Avidin-conjugated beads were used to pull down labeled proteins. Unlabeled $\alpha_3\beta_1$ integrin in the supernatant was immunoprecipitated with the polyclonal anti–α_3 integrin antibody.

Isolation of Golgi fraction. Isolation of Golgi fraction from cultured *Pkd1*$^{+/+}$ and *Pkd1*$^{-/-}$ cells was done by using a discontinuous sucrose gradient ultracentrifugation described by Balch et al. (65). Briefly, confluent cells were harvested and washed in homogenization medium (10 mM Tris/HCl, pH 7.4, 250 mM sucrose) 2 times and homogenized in 3 ml homogenization medium, with sucrose concentration adjusted to 1.4 M. Sample solution (3.9 ml) was transferred to an approximately 11-ml ultracentrifuge tube, and the sample was overlaid with 3.9 ml of 1.2 M sucrose gradient solution and then 1.95 ml of 0.8 M sucrose gradient solution. A syringe was used to underlay the sample with 1.3 ml of 1.6 M sucrose gradient solution. Centrifugation was carried out at 4°C, 110,000 *g*, for 2 hours. The Golgi fraction band was harvested from the 0.8 M/1.2 M sucrose interface.

Real-time PCR. Real-time PCR was carried out on a Smart Cycler II (Cepheid). SyBR Green was used for fluorescence detection. PCR parameters were 95°C, 10 minutes (95°C, 15 seconds, 60°C, 30 seconds, 72°C, 30 seconds) 40 cycles; melting temperature was measured between 60 and 95°C. c-Met forward primer was ACGGCTGAAGGAAACCCAAG; reverse primer, ACCCAGAGTCTACGGAACAGA. The *c-Met* mRNA amount was normalized by the 18S RNA amount from the same cDNA sample.

Glycosylation analysis. WT and *Pkd1*$^{-/-}$ cells were lysed and incubated with Endo H and PNGase F glycosidase enzymes (New England Biolabs), following the manufacturer's instructions for the digestion. Western blot analysis under reducing conditions with antibody against the C terminus of α_3 integrin was used to evaluate the migration change before and after Endo-H and PNGase F digestion.

Organ culture in vitro. Embryonic mouse kidneys of E13.5 were dissected out and cultured in media (30) (1% FBS, 5 mg/ml transferrin, 0.05 mM sodium selenite, 100 nM hydrocortisone, 2 nM T3, 25 ng/ml PGE_1, 100 U/ml penicillin/streptomycin, 100 μM 8-Br-cAMP) in a Center-Well Organ Culture Dish (BD Labware). The following day, the kidneys from the same embryo were treated with either 5 mM Met Kinase Inhibitor (Calbiochem) or DMSO (the same volume as Met Kinase Inhibitor). The media were changed every day with the same additives as above. After 5 days, kidneys were fixed by 4% PFA and embedded in paraffin. Paraffin sections were stained with hematoxylin and eosin.

Treatment of pregnant mice. Male and female *Pkd1*$^{+/-}$ mice were intercrossed to obtain homozygous mutant embryos. At E14.5, pregnant *Pkd1*$^{+/-}$ females received intraperitoneally injections of either c-Met kinase inhibitor (Calbiochem 448101) or vehicle. c-Met kinase inhibitor was dissolved in 30% DMSO/20% ethanol/50% PBS (vehicle) and injected at an amount of 100 mg/kg/d, divided into two doses, one in the morning and the other in the evening. The pregnant mice were injected at E14.5, E15.5, E16.5, and E17.5 and sacrificed at E18.5. The E18.5 embryonic kidneys were fixed in 4% PFA and genotyped, and paraffin sections were obtained and stained with hematoxylin and eosin. Cyst area was analyzed on a Nikon Eclipse 80i microscope and quantified by NIS-Elements software (Nikon Instech Co.).

Statistics. All data are presented as mean ± SEM. Student's 2-tailed *t* test for unpaired groups was used to compare the mean of different groups. The difference between 2 means was significant when *P* was lees than 0.01.

Acknowledgments

J.A. Kreidberg acknowledges support from NIH grants DK50118-01 and P50DK074030. S. Qin was supported by a Scientist Development Grant 09SDG2170031 from the American Heart Association and Fellowship Grant 180F08b from the PKD Foundation. J. Zhou acknowledges support from NIH grants P50DK074030, DK51050, DK074030, and DK40703. The authors thank Helmut Rennke for providing samples of human PKD kidneys and Valerie Schumacher, Jacqueline Ho, and Sunny Hartwig for valuable discussions.

Received for publication October 21, 2009, and accepted in revised form July 28, 2010.

Address correspondence to: Jordan Kreidberg, Division of Nephrology, Children's Hospital, 300 Longwood Avenue, Boston, Massachusetts 02115, USA. Phone: 617.919.2959; Fax: 617.730.0129; E-mail: Jordan.Kreidberg@childrens.harvard.edu.

1. Lu W, et al. Late onset of renal and hepatic cysts in Pkd1-targeted heterozygotes. *Nat Genet*. 1999;21(2):160–161.
2. Mochizuki T, et al. PKD2, a gene for polycystic kidney disease that encodes an integral membrane protein. *Science*. 1996;272(5266):1339–1342.
3. Igarashi P, Somlo S. Polycystic kidney disease. *J Am Soc Nephrol*. 2007;18(5):1371–1373.
4. Nakamura T, et al. Growth factor gene expression in kidney of murine polycystic kidney disease. *J Am Soc Nephrol*. 1993;3(7):1378–1386.
5. Matsell DG, Bennett T, Armstrong RA, Goodyer P, Goodyer C, Han VK. Insulin-like growth factor (IGF) and IGF binding protein gene expression in multicystic renal dysplasia. *J Am Soc Nephrol*. 1997;8(1):85–94.
6. Horie S, et al. Mediation of renal cyst formation by hepatocyte growth factor. *Lancet*. 1994;344(8925):789–791.
7. Sullivan LP, et al. Sulfonylurea-sensitive K(+) transport is involved in Cl(-) secretion and cyst growth by cultured ADPKD cells. *J Am Soc Nephrol*. 2002;13(11):2619–2627.
8. Leipziger J. Control of epithelial transport via luminal P2 receptors. *Am J Physiol Renal Physiol*. 2003;284(3):F419–432.
9. Joly D, Berissi S, Bertrand A, Strehl L, Patey N, Knebelmann B. Laminin 5 regulates polycystic kidney cell proliferation and cyst formation. *J Biol Chem*. 2006;281(39):29181–29189.
10. Malhas AN, Abuknesha RA, Price RG. Interaction of the leucine-rich repeats of polycystin-1 with extracellular matrix proteins: possible role in cell proliferation. *J Am Soc Nephrol*. 2002;13(1):19–26.
11. Kovacs J, Carone FA, Liu ZZ, Nakumara S, Kumar A, Kanwar YS. Differential growth factor-induced

modulation of proteoglycans synthesized by normal human renal versus cyst-derived cells. *J Am Soc Nephrol*. 1994;5(1):47–54.
12. Pachnis V, Mankoo B, Costantini F. Expression of the c-ret proto-oncogene during mouse embryogenesis. *Development*. 1993;119(4):1005–1017.
13. Dudley AT, Godin RE, Robertson EJ. Interaction between FGF and BMP signaling pathways regulates development of metanephric mesenchyme. *Genes Dev*. 1999;13(12):1601–1613.
14. Kuo NT, Norman JT, Wilson PD. Acidic FGF regulation of hyperproliferation of fibroblasts in human autosomal dominant polycystic kidney disease. *Biochem Mol Med*. 1997;61(2):178–191.
15. Santos OF, et al. Involvement of hepatocyte growth factor in kidney development. *Dev Biol*. 1994;163(2):525–529.
16. Santos OF, Nigam SK. HGF-induced tubulogenesis and branching of epithelial cells is modulated by extracellular matrix and TGF-beta. *Dev Biol*. 1993;160(2):293–302.
17. Konda R, Sato H, Hatafuku F, Nozawa T, Ioritani N, Fujioka T. Expression of hepatocyte growth factor and its receptor C-met in acquired renal cystic disease associated with renal cell carcinoma. *J Urol*. 2004;171(6 pt 1):2166–2170.
18. Kreidberg JA, et al. Alpha 3 beta 1 integrin has a crucial role in kidney and lung organogenesis. *Development*. 1996;122(11):3537–3547.
19. Shannon MB, Patton BL, Harvey SJ, Miner JH. A hypomorphic mutation in the mouse laminin alpha5 gene causes polycystic kidney disease. *J Am Soc Nephrol*. 2006;17(7):1913–1922.
20. Chang JC, Chang HH, Lin CT, Lo SJ. The integrin alpha6beta1 modulation of PI3K and Cdc42 activities induces dynamic filopodium formation in human platelets. *J Biomed Sci*. 2005;12(6):881–898.
21. Tang K, Nie D, Cai Y, Honn KV. The beta4 integrin subunit rescues A431 cells from apoptosis through a PI3K/Akt kinase signaling pathway. *Biochem Biophys Res Commun*. 1999;264(1):127–132.
22. Shillingford JM, et al. The mTOR pathway is regulated by polycystin-1, and its inhibition reverses renal cystogenesis in polycystic kidney disease. *Proc Natl Acad Sci U S A*. 2006;103(14):5466–5471.
23. Nauli SM, et al. Loss of polycystin-1 in human cyst-lining epithelia leads to ciliary dysfunction. *J Am Soc Nephrol*. 2006;17(4):1015–1025.
24. Abella JV, et al. Met/Hepatocyte growth factor receptor ubiquitination suppresses transformation and is required for Hrs phosphorylation. *Mol Cell Biol*. 2005;25(21):9632–9645.
25. Nath D, Williamson NJ, Jarvis R, Murphy G. Shedding of c-Met is regulated by crosstalk between a G-protein coupled receptor and the EGF receptor and is mediated by a TIMP-3 sensitive metalloproteinase. *J Cell Sci*. 2001;114(pt 6):1213–1220.
26. Kaabeche K, Guenou H, Bouvard D, Didelot N, Listrat A, Marie PJ. Cbl-mediated ubiquitination of alpha5 integrin subunit mediates fibronectin-dependent osteoblast detachment and apoptosis induced by FGFR2 activation. *J Cell Sci*. 2005; 118(pt 6):1223–1232.
27. Liu Y, et al. Coordinate integrin and c-Met signaling regulate Wnt gene expression during epithelial morphogenesis. *Development*. 2009;136(5):843–853.
28. Wang Z, Symons JM, Goldstein SL, McDonald A, Miner JH, Kreidberg JA. (Alpha)3(beta)1 integrin regulates epithelial cytoskeletal organization. *J Cell Sci*. 1999;112(pt 17):2925–2935.
29. Charron AJ, Nakamura S, Bacallao R, Wandinger-Ness A. Compromised cytoarchitecture and polarized trafficking in autosomal dominant polycystic kidney disease cells. *J Cell Biol*. 2000;149(1):111–124.
30. Magenheimer BS, et al. Early embryonic renal tubules of wild-type and polycystic kidney disease kidneys respond to cAMP stimulation with cystic fibrosis transmembrane conductance regulator/Na(+),K(+),2Cl(-) Co-transporter-dependent cystic dilation. *J Am Soc Nephrol*. 2006;17(12):3424–3437.
31. Meyer RB Jr, Miller JP. Analogs of cyclic AMP and cyclic GMP: general methods of synthesis and the relationship of structure to enzymic activity. *Life Sci*. 1974;14(6):1019–1040.
32. Kasagi Y, Horiba N, Sakai K, Fukuda Y, Suda T. Involvement of cAMP-response element binding protein in corticotropin-releasing factor (CRF)-induced down-regulation of CRF receptor 1 gene expression in rat anterior pituitary cells. *J Neuroendocrinol*. 2002;14(7):587–592.
33. Takayama H, LaRochelle WJ, Sabnis SG, Otsuka T, Merlino G. Renal tubular hyperplasia, polycystic disease, and glomerulosclerosis in transgenic mice overexpressing hepatocyte growth factor/scatter factor. *Lab Invest*. 1997;77(2):131–138.
34. Bukanov NO, Smith LA, Klinger KW, Ledbetter SR, Ibraghimov-Beskrovnaya O. Long-lasting arrest of murine polycystic kidney disease with CDK inhibitor roscovitine. *Nature*. 2006;444(7121):949–952.
35. Lanoix J, D'Agati V, Szabolcs M, Trudel M. Dysregulation of cellular proliferation and apoptosis mediates human autosomal dominant polycystic kidney disease (ADPKD). *Oncogene*. 1996;13(6):1153–1160.
36. Torres VE. Role of vasopressin antagonists. *Clin J Am Soc Nephrol*. 2008;3(4):1212–1218.
37. Shibazaki S, et al. Cyst formation and activation of the extracellular regulated kinase pathway after kidney specific inactivation of Pkd1. *Hum Mol Genet*. 2008;17(11):1505–1516.
38. Happe H, et al. Toxic tubular injury in kidneys from Pkd1-deletion mice accelerates cystogenesis accompanied by dysregulated planar cell polarity and canonical Wnt signaling pathways. *Hum Mol Genet*. 2009;18(14):2532–2542.
39. Takakura A, Contrino L, Beck AW, Zhou J. Pkd1 inactivation induced in adulthood produces focal cystic disease. *J Am Soc Nephrol*. 2008;19(12):2351–2363.
40. Ohnishi H, Mizuno S, Nakamura T. Inhibition of tubular cell proliferation by neutralizing endogenous HGF leads to renal hypoxia and bone marrow-derived cell engraftment in acute renal failure. *Am J Physiol Renal Physiol*. 2008;294(2):F326–335.
41. Ramos-Nino ME, et al. HGF mediates cell proliferation of human mesothelioma cells through a PI3K/MEK5/Fra-1 pathway. *Am J Respir Cell Mol Biol*. 2008;38(2):209–217.
42. Piontek K, Menezes LF, Garcia-Gonzalez MA, Huso DL, Germino GG. A critical developmental switch defines the kinetics of kidney cyst formation after loss of Pkd1. *Nat Med*. 2007;13(12):1490–1495.
43. Lelongt B, Carone FA, Kanwar YS. Decreased de novo synthesis of proteoglycans in drug-induced renal cystic disease. *Proc Natl Acad Sci U S A*. 1988; 85(23):9047–9051.
44. Jin H, Carone FA, Nakamura S, Liu ZZ, Kanwar YS. Altered synthesis and intracellular transport of proteoglycans by cyst-derived cells from human polycystic kidneys. *J Am Soc Nephrol*. 1992;2(12):1726–1733.
45. Ehara T, Carone FA, McCarthy KJ, Couchman JR. Basement membrane chondroitin sulfate proteoglycan alterations in a rat model of polycystic kidney disease. *Am J Pathol*. 1994;144(3):612–621.
46. Beavan LA, Carone FA, Nakamura S, Jones JK, Reindel JF, Price RG. Comparison of proteoglycans synthesized by porcine normal and polycystic renal tubular epithelial cells in vitro. *Arch Biochem Biophys*. 1991;284(2):392–399.
47. Charron AJ, Bacallao RL, Wandinger-Ness A. ADPKD: a human disease altering Golgi function and basolateral exocytosis in renal epithelia. *Traffic*. 2000;1(8):675–686.
48. Carone FA, Jin H, Nakamura S, Kanwar YS. Decreased synthesis and delayed processing of sulfated glycoproteins by cells from human polycystic kidneys. *Lab Invest*. 1993;68(4):413–418.
49. Aydar E, Palmer CP. Polycystic kidney disease channel and synaptotagmin homologues play roles in schizosaccharomyces pombe cell wall synthesis/repair and membrane protein trafficking. *J Membr Biol*. 2009;229(3):141–152.
50. Lai AZ, Abella JV, Park M. Crosstalk in Met receptor oncogenesis. *Trends Cell Biol*. 2009;19(10):542–551.
51. Bacallao RL, McNeill H. Cystic kidney diseases and planar cell polarity signaling. *Clin Genet*. 2009;75(2):107–117.
52. Fischer E, et al. Defective planar cell polarity in polycystic kidney disease. *Nat Genet*. 2006;38(1):21–23.
53. Saburi S, et al. Loss of Fat4 disrupts PCP signaling and oriented cell division and leads to cystic kidney disease. *Nat Genet*. 2008;40(8):1010–1015.
54. Patel V, et al. Acute kidney injury and aberrant planar cell polarity induce cyst formation in mice lacking renal cilia. *Hum Mol Genet*. 2008;17(11):1578–1590.
55. Apte U, et al. Activation of Wnt/beta-catenin pathway during hepatocyte growth factor-induced hepatomegaly in mice. *Hepatology*. 2006;44(4):992–1002.
56. Yu W, O'Brien LE, Wang F, Bourne H, Mostov KE, Zegers MM. Hepatocyte growth factor switches orientation of polarity and mode of movement during morphogenesis of multicellular epithelial structures. *Mol Biol Cell*. 2003;14(2):748–763.
57. Yoder BK. Role of primary cilia in the pathogenesis of polycystic kidney disease. *J Am Soc Nephrol*. 2007;18(5):1381–1388.
58. Yoder BK, Hou X, Guay-Woodford LM. The polycystic kidney disease proteins, polycystin-1, polycystin-2, polaris, and cystin, are co-localized in renal cilia. *J Am Soc Nephrol*. 2002;13(10):2508–2516.
59. Poole CA, Zhang ZJ, Ross JM. The differential distribution of acetylated and detyrosinated alpha-tubulin in the microtubular cytoskeleton and primary cilia of hyaline cartilage chondrocytes. *J Anat*. 2001;199(pt 4):393–405.
60. Follit JA, Tuft RA, Fogarty KE, Pazour GJ. The intraflagellar transport protein IFT20 is associated with the Golgi complex and is required for cilia assembly. *Mol Biol Cell*. 2006;17(9):3781–3792.
61. Tenkova T, Chaldakov GN. Golgi-cilium complex in rabbit ciliary process cells. *Cell Struct Funct*. 1988;13(5):455–458.
62. Girod C, Lheritier M, Guichard Y. (Cilia-centriole-Golgi apparatus relationships in the glandular cells of the anterior pituitary of the hedgehog [Erinaceus europaeus L]). *C R Seances Acad Sci D*. 1980;290(11):711–714.
63. Chattopadhyay N, Wang Z, Ashman LK, Brady-Kalnay SM, Kreidberg JA. alpha3beta1 integrin-CD151, a component of the cadherin-catenin complex, regulates PTPmu expression and cell-cell adhesion. *J Cell Biol*. 2003;163(6):1351–1362.
64. Nauli SM, Kawanabe Y, Kaminski JJ, Pearce WJ, Ingber DE, Zhou J. Endothelial cilia are fluid shear sensors that regulate calcium signaling and nitric oxide production through polycystin-1. *Circulation*. 2008;117(9):1161–1171.
65. Balch WE, Dunphy WG, Braell WA, Rothman JE. Reconstitution of the transport of protein between successive compartments of the Golgi measured by the coupled incorporation of N-acetylglucosamine. *Cell*. 1984;39(2 pt 1):405–416.